

HOSTED BY



ELSEVIER

Contents lists available at ScienceDirect

Engineering Science and Technology, an International Journal

journal homepage: www.elsevier.com/locate/jestch

Full Length Article

Design and analysis of a novel concentric rings based crossed lines single negative metamaterial structure

Adham R. Azeez^a, Taha A. Elwi^{b,*}, Zaid A. Abed AL-Hussain^a^a Department of Electrical Engineering, Al-Mustansiriya University, Baghdad, Iraq^b Department of Communication Engineering, Al-Mammon University Collage, Baghdad, Iraq

ARTICLE INFO

Article history:

Received 5 August 2016

Revised 2 November 2016

Accepted 11 November 2016

Available online xxx

Keywords:

CR-CL MTM

NRW

FEM

Circuit analysis

ABSTRACT

This paper presents the design and analysis of a novel single negative metamaterial (MTM) based on concentric rings with crossed lines (CR-CL) to be miniaturized to $\lambda/4$ at 15G Hz. The unit cell is structured to behave as a single negative MTM, $-\epsilon$ or $-\mu$, at different frequency bands. The unit cell is consistent of a dielectric substrate, $5 \times 5 \times 1 \text{ mm}^3$, of FR4-Epoxy underneath of a conductive patch designed as $4.4 \times 4.4 \text{ mm}^2$. A complete analysis in terms of S-parameters, constitutive parameters and refraction index are evaluated for the unit cell using both full wave simulation and circuitry analysis as well. Nevertheless, the unit cell characteristics based circuit equivalent lumped components are retrieved. HFSS software package based on Finite Element Method (FEM) and Advanced Design System (ADS) based on circuit analysis formulations are invoked to perform the simulation study. Later on, the obtained simulation results are compared to their identical measurements based on transmission line technique. Finally, the simulated and measured results are agreed excellently.

© 2016 Karabuk University. Publishing services by Elsevier B.V. This is an open access article under the CC BY-NC-ND license (<http://creativecommons.org/licenses/by-nc-nd/4.0/>).

1. Introduction

MTM structures are defined as artificial materials that show unique properties, after engineering them in certain sets, not found in the nature [1]. The properties of MTM depend on the shape, orientation, arrangement and size of the inclusion [2]. In 1967, the Russian physicist, Viktor Veselago, attracted the attentions to $-\epsilon$ and $-\mu$ to be called left hand materials [3]. Veselago showed these materials can make phase velocity anti-parallel to the direction of the Poynting vector to be opposed to the wave propagation [3]. Later, John Pendry introduced the first practical MTM prototype [4] based on arrays of wires along the direction of wave propagation to provide $-\epsilon$. In 1999, Pendry succeed to implement a structure with $-\mu$ by introducing metal Split Ring Resonators (SRR) arrayed in the parallel direction to the wave propagation [5]. Smith *et al.* mixed the arrays of wires with the SRR together on the same substrate to provide $-\epsilon$ and $-\mu$ [6].

In all previous researches, the proposed MTM structures suffered from obvious losses due to adding either via or shorting wire

structures, however, this research proposes a novel MTM structure to produce single negative electromagnetic properties type of $-\mu$ besides to $-\epsilon$ at separate bands without the need for adding via or wire structures. The proposed unit cell geometry is provided in section two. In section three, the numerical and analytical results are discussed. The validation of the obtained results is measured with a practical prototype in section four. Finally, the paper is concluded in section five.

2. CR-CL MTM geometrical details

In Fig. 1, the unit cell geometry is presented. The proposed unit cell is constructed from a dielectric FR4-Epoxy substrate and copper patch. The substrate ϵ_r is 4.4 and $\tan \delta$ is 0.02. The copper patch dimensions are $4.4 \times 4.4 \text{ mm}^2$ printed on the substrate. The other related geometrical details are provided in Fig. 1.

3. CR-CL MTM analysis

3.1. Full wave analysis

The unit cell electromagnetic characteristics interms of S-parameters, constitutive parameters and refraction index are per-

* Corresponding author.

E-mail address: taelwi82@gmail.com (T.A. Elwi).

Peer review under responsibility of Karabuk University.

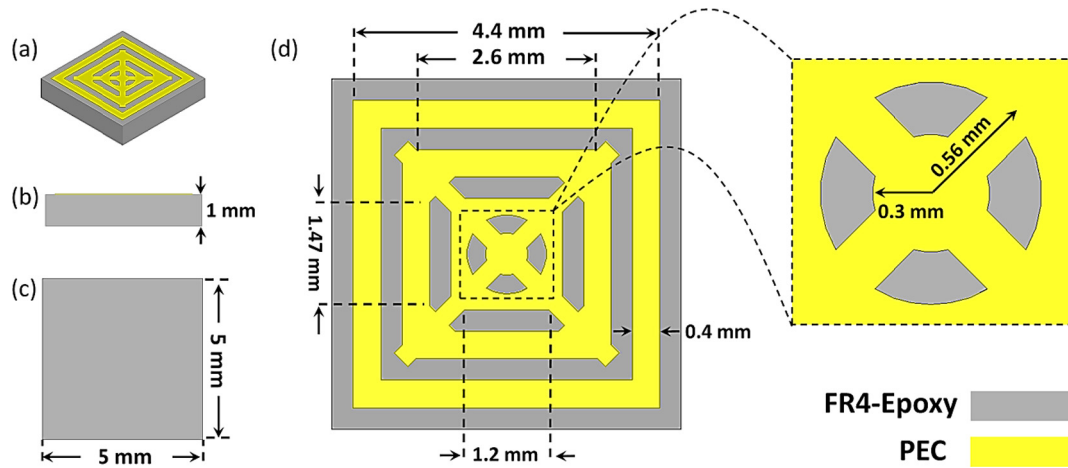


Fig. 1. Shaped and dimensions of CR-CL MTM: (a) 3D view, (b) Side view, (c) back view, and (d) Top view.

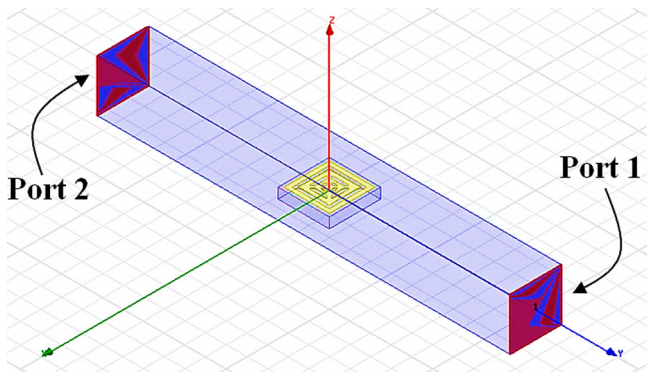


Fig. 2. The fictitious waveguide with excitation ports.

formed in this section. The evaluated numerical results are obtained from the FEM analysis based on HFSS formulations and Matlab codes.

3.1.1. Constitutive parameters retrieving

The unit cell is inserted inside a fictitious waveguide to retrieve the S-parameters. At the $\pm y$ planes of the waveguide two ports are applied as shown in Fig. 2. To mimic the behavior of infinite arrays of the unit cell, perfect electrical conductors (PECs) are assigned in the $\pm x$ directions of the waveguide, while perfect magnetic conductors (PMCs) are applied along the $\pm z$ directions. Fig. 3 shows the S-parameters in term of magnitude and phase.

To find the constitutive parameters, μ_r and ϵ_r , the evaluated S-parameters are imported to a Matlab code retriever based Nicolson-Ross-Weir (NRW) technique. Eqs. (1) and (2) are used

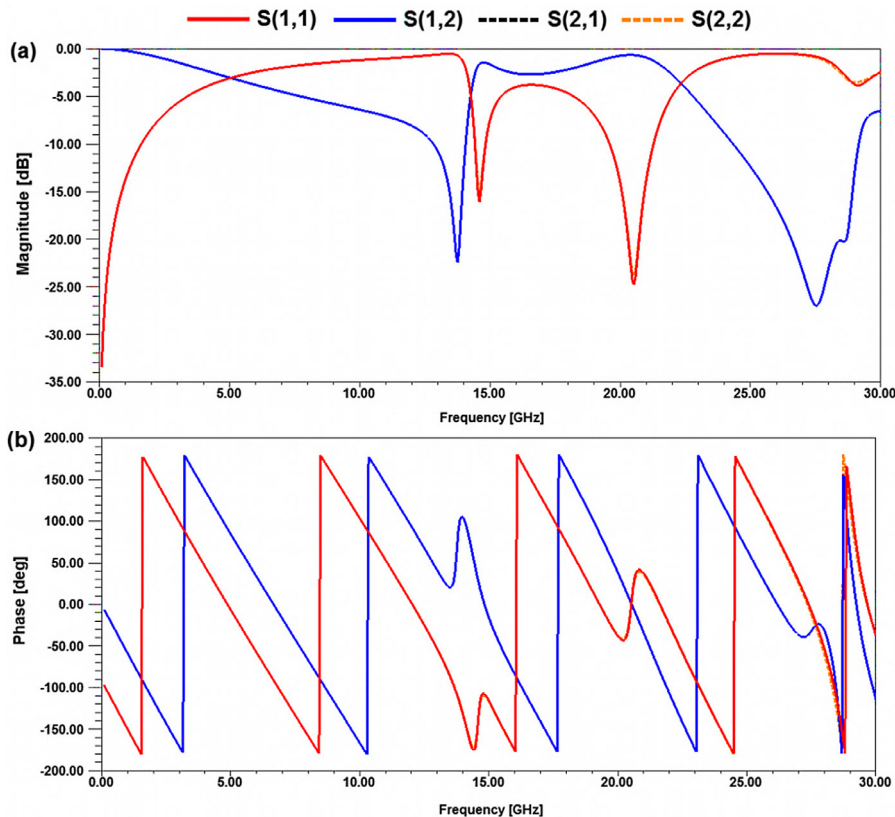


Fig. 3. The S-parameters of CR-CL MTM: (a) Magnitude and (b) Phase.

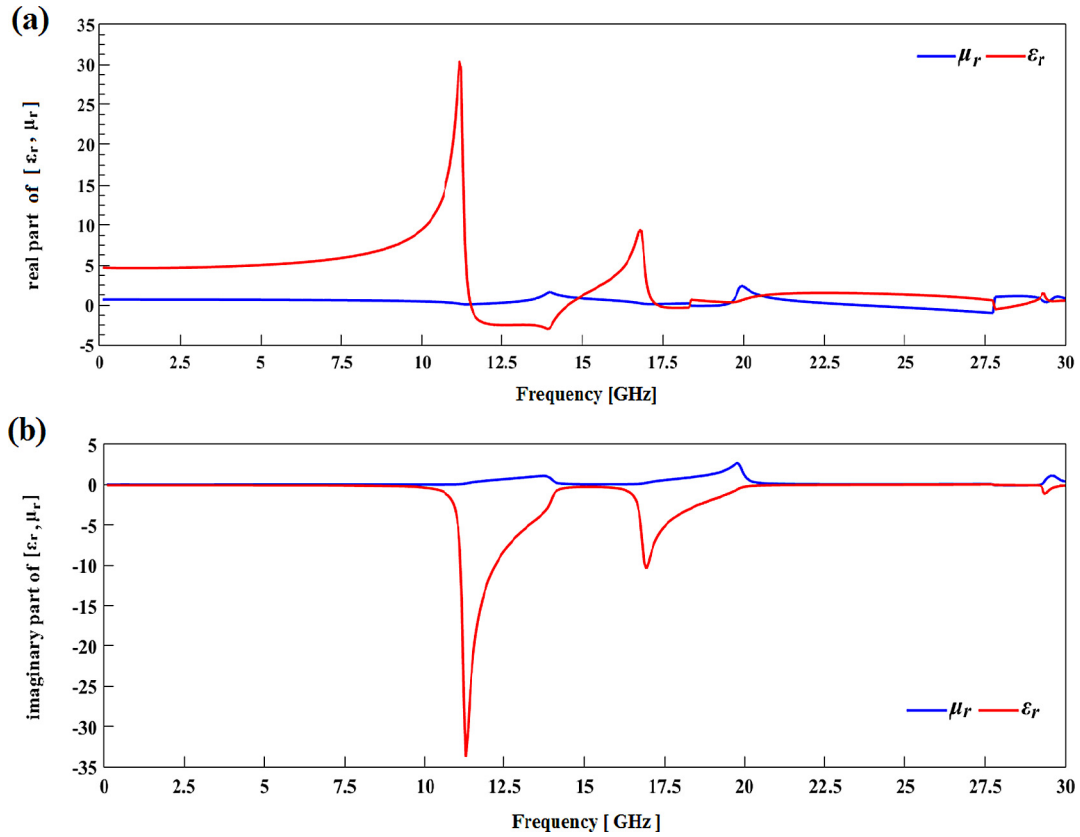


Fig. 4. The retrieved ϵ_r and μ_r : (a) Real part and (b) Imaginary part.

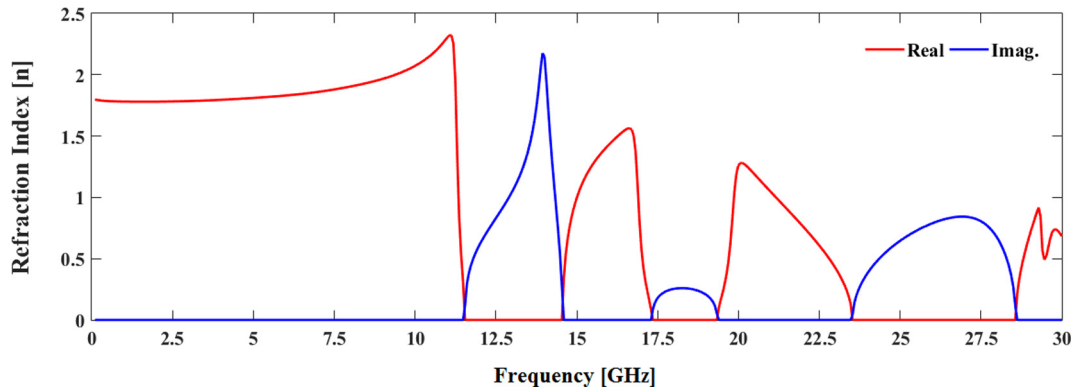


Fig. 5. The retrieved n in terms of real and imaginary.

to evaluate the constitutive parameters based on NRW technique [7].

$$\mu_r = \frac{2c(1 - V_2)}{\omega i(1 + V_2)d} \quad (1)$$

$$\epsilon_r = \mu_r + i \frac{2S_{11}c}{\omega d} \quad (2)$$

where c is the speed of light, ω is the angular frequency, d is the substrate thickness and V_2 is the voltage minima where equals to $S_{21} - S_{11}$.

In Fig. 4, the obtained constitutive parameters are presented. It is found that the proposed CR-CL structure shows $-\epsilon_r$ and $-\mu_r$ at different frequency bands. Where, the negative ϵ_r can be found at the frequency ranges from 11.66 GHz to 14.45 GHz, 17.35 GHz to 18.31 GHz and 27.78 GHz to 28.56 GHz, while, the negative μ_r found at 18.37 GHz to 19.33 GHz and 23.52 GHz to 27.72 GHz.

To retrieve the refractive index (n), Eq. (3) is used [3]. It is obvious from Fig. 5 that the proposed unit cell shows an imaginary n when μ or ϵ is negative value only.

$$n = \sqrt{\epsilon_r \mu_r} \quad (3)$$

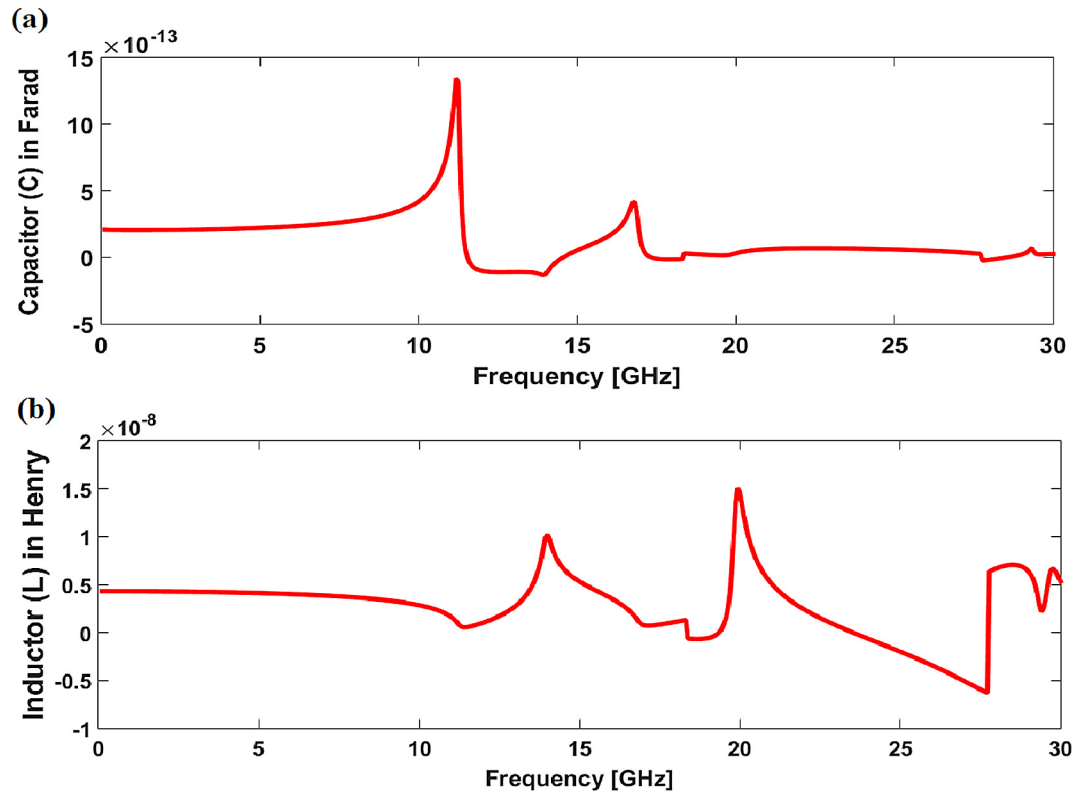


Fig. 6. The retrieved equivalent lumped elements: (a) Capacitor and (b) Inductor.

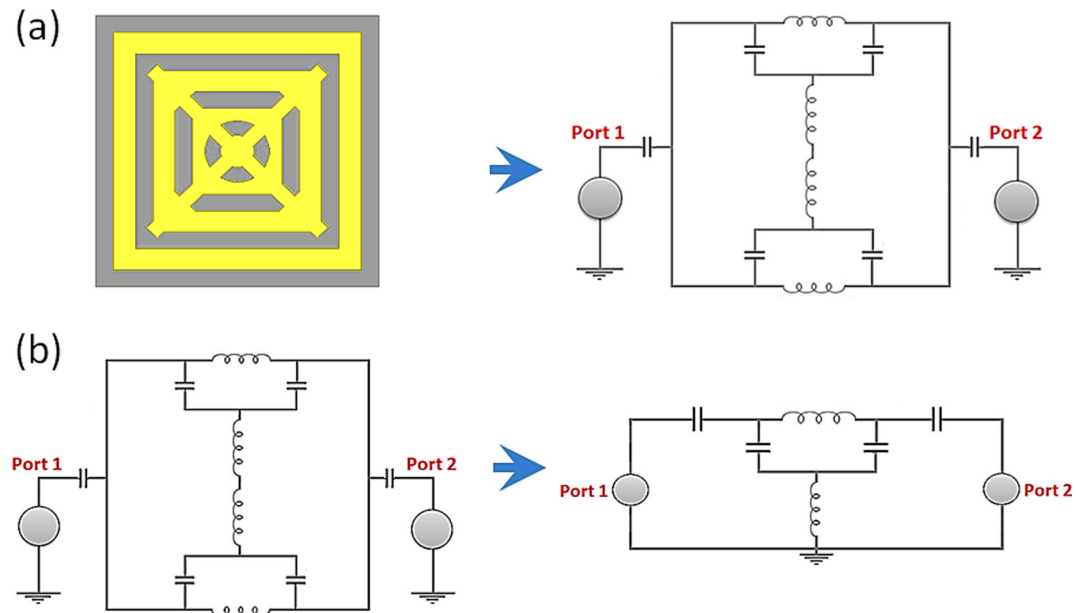


Fig. 7. The equivalent circuit (a) MTM unit cell circuit before simplification and (b) the simplified equivalent circuit.

3.1.2. Description the CR-CL MTM properties in terms of lumped elements

A new description for the electromagnetic parameters is applied in this work. The proposed unit cell properties are described in terms of lumped elements instead of constitutive parameters. The lumped elements interms of L and C are evaluated by multiply-

ing the constitutive parameters by the unit cell size. Fig. 6 shows the dispersion spectra variation of both C and L with respect to the frequency.

The new description of proposed MTM shows negative values of both C and L over certain bands, while, it shows positive values over other bands.

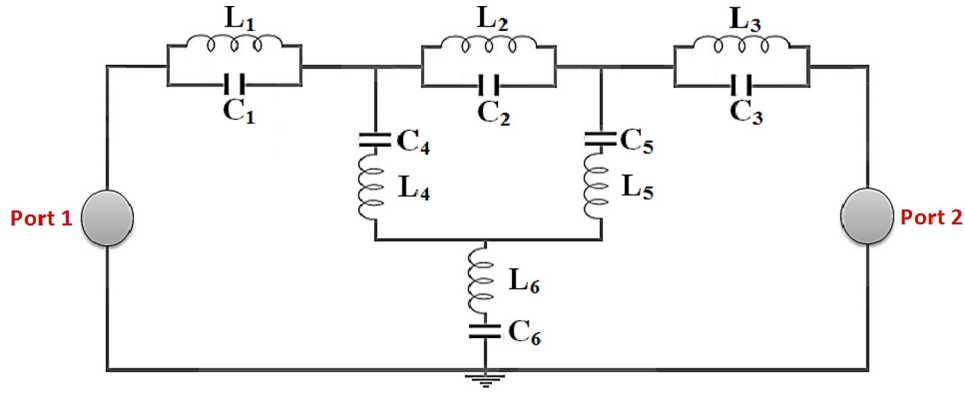


Fig. 8. Composite unit cell MTM configuration.

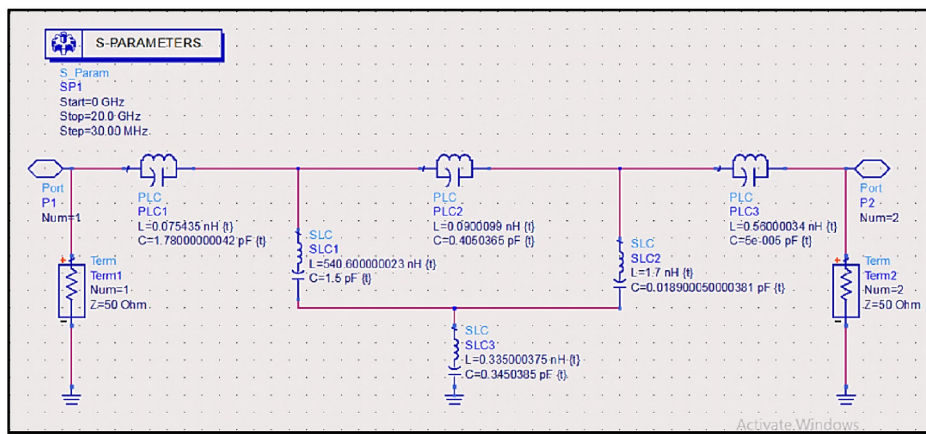


Fig. 9. The MTM unit cell modeling inside the ADS schematic window.

Table 1
Lumped elements values of the Unit cell Equivalent Circuit.

Element	Inductor (nH)						Capacitor (pF)						
	Symbol	L ₁	L ₂	L ₃	L ₄	L ₅	L ₆	C ₁	C ₂	C ₃	C ₄	C ₅	C ₆
Value		0.075	0.090	0.560	540.6	1.7	0.335	1.780	0.405	0.00005	1.5	0.018	0.345

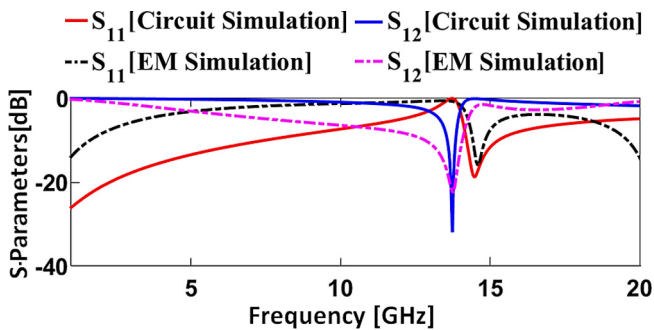


Fig. 10. Comparison between Circuit Simulation and EM simulation.

3.2. Transmission line model

A transmission line model (TLM) is applied to describe the equivalent circuit of the proposed unit cell using lumped elements. From the MTM unit cell geometry, the equivalent circuit is derived

as shown in Fig. 7(a). The inductor presents the metallic strips and the capacitor presents the air gaps between these strips [7]. Then, the equivalent circuit of the proposed unit cell has been simplified as shown in Fig. 7(b).

The last equivalent circuit, the simplified one, presents a purely single negative MTM behavior. Unfortunately, the pure MTM structures over a wideband frequency are not exist in reality due to the parasitic effects which are unavoidable and as a result, the composite MTM equivalent circuit model is presented as seen in Fig. 8.

The equivalent circuit is designed using TLM based on ADS environments as seen in Fig. 9. The values of the circuit components, L and C, are tuned to achieve S-parameters spectra close to those evaluated from the full wave analysis. Table 1 shows the values of the circuit components L and C.

The obtained results from the equivalent circuit in the ADS environment is compared to the 3D simulated results in terms of S-parameters spectra. It is found there is a good agreement with a slight difference between the circuit simulation and EM simulation as seen in Fig. 10. This difference is attributed to the diffraction

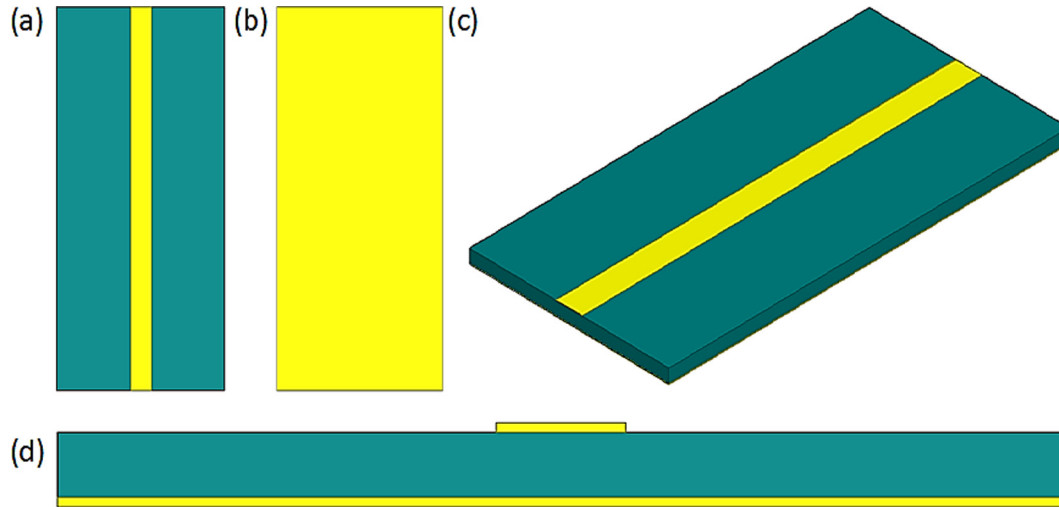


Fig. 11. Microstrip Line Geometry: (a) Top view, (b) Bottom view, (c) 3D view, (d) Front view.



Fig. 12. MSTL based CR-CL MTM (MSM).

effects, substrate and conductive loss, fringing effects and the exact geometrical details that are ignored in the circuit simulations while they are included in the EM simulation model.

4. Validation and measurements

A microstrip line is conducted to study the performance of the proposed unit cell. This technique is based on evaluating the S-parameters of the transmission line with and without adding the unit cell. The proposed microstrip line that shown in Fig. 11 is designed inside HFSS environments. The microstrip line is consistent of a transmission line of copper, $30 \times 1.926 \text{ mm}^2$, mounted on an FR4 substrate with dimensions of $30 \times 15 \text{ mm}^2$ and thickness 1 mm backed with a ground plane.

Then, the proposed unit cell is added to the same microstrip line as seen in Fig. 12 to study the performance of the MTM structure.

In Fig. 13, the simulated S-parameters of the microstrip line with and without MTM unit cell are presented.

Now, to verify of veracity of simulated results, a microstrip line is fabricated based MTM unit cell and both of S_{11} and S_{21} spectra are measured. Fig. 14 shows the fabricated prototype and the measuring process.

As seen in Fig. 15, the experimental results are compared to the simulated results. It is found an excellent agreement that is achieved between simulated and measured results with insignificant difference due to the soldering defects.

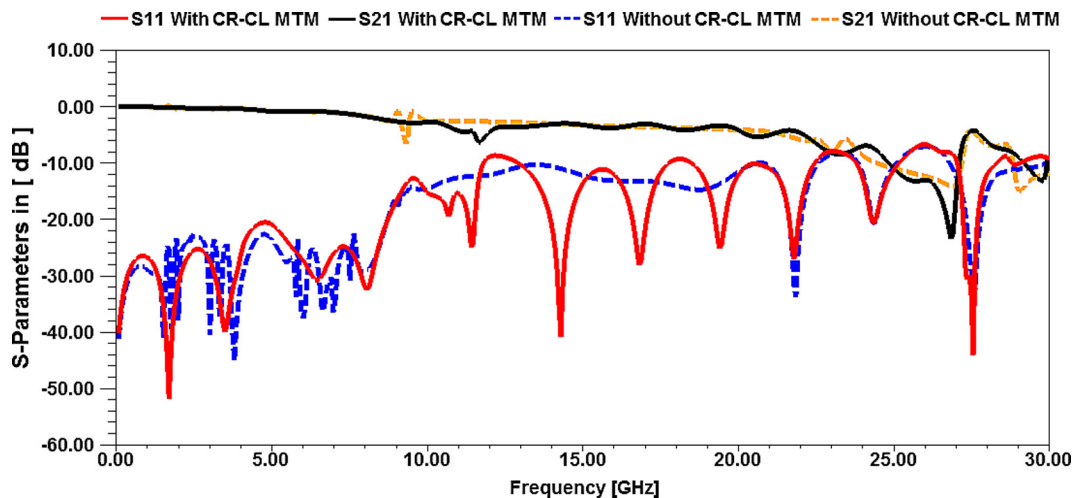


Fig. 13. Comparison the simulated S_{11} and S_{21} before and after added MTM unit cell.

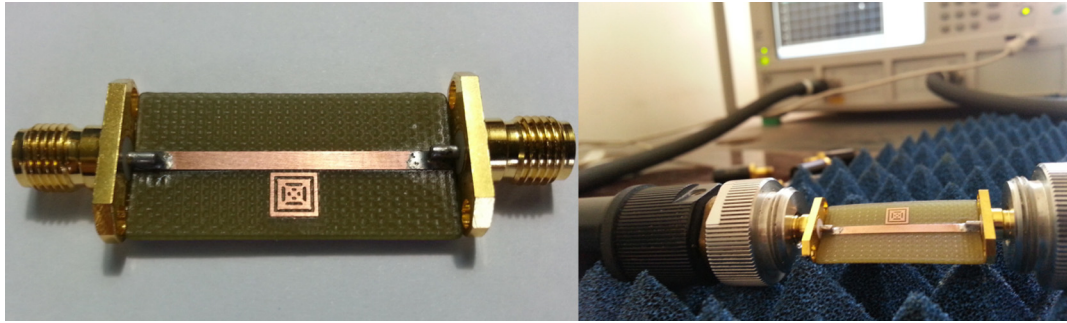


Fig. 14. The MSM fabrication and measurement process with two SMA connectors.

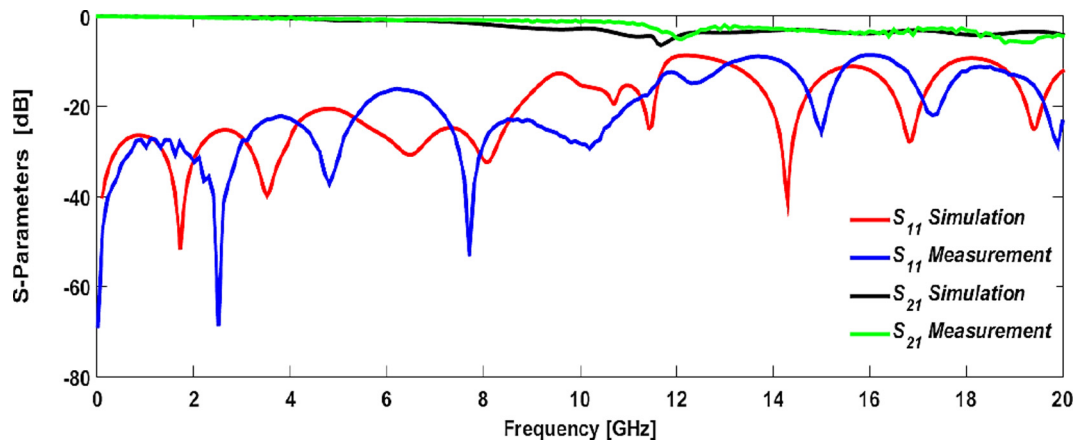


Fig. 15. Comparison between simulation and measurement results.

5. Conclusion

A novel MTM structure based on concentric rings with crossed lines unit cell is presented to provide a $-\mu$ besides to $-\varepsilon$ without the need to conduct via or wires. The proposed unit cell is designed using 3D full wave simulator based HFSS and re-evaluated using TLM based on ADS formulations. It is found the proposed MTM structure shows a $-\varepsilon_r$ over the frequency bands 11.66–14.45 GHz, 17.35–18.31 GHz and 27.78–28.56 GHz, while the $-\mu_r$ is found at 18.37–19.33 GHz and 23.52–27.72 GHz. Nevertheless, the performance of the proposed MTM is tested experimentally by launching a single unit cell to a microstrip line and measuring the S-parameters spectra, then, comparing the achieved results to the simulated results. The electromagnetic constitutive parameters and the equivalent circuit model elements are retrieved. An excellent agreement is achieved between the simulated and measured results.

References

- [1] T.A. Elwi, Z. Abbas, M.A. Elwi, M.M. Hamed, On the performance of the 2D planar metamaterial structure, *Int. J. Electron. Commun.* 68 (9) (2014) 846–850.
- [2] T.A. Elwi, A further investigation on the performance of the broadside coupled rectangular split ring resonators, *Prog. Electromagn. Res. Lett.* 34 (2012) 1–8.
- [3] Taha A. Elwi, A.I. Imran, Y. Alnaiemy, A miniaturized lotus shaped microstrip antenna loaded with EBG structures for high gain-bandwidth product applications, *Prog. Electromagn. Res. C* 60 (2015) 157–167.
- [4] B. Sauviac, C.R. Simovski, S.A. Tretyakov, Double split-ring resonators: analytical modeling and numerical simulations, *Electromagnetics* 24 (5) (2004) 317–338.
- [5] J.D. Baena, R. Marques, F. Medina, J. Martel, Artificial magnetic metamaterial design by using spiral resonators, *Phys. Rev. B* 69 (2004) 0144021–0144025.
- [6] H. Chen, L. Ran, J. Huangfu, X. Zhang, K. Chen, Left-handed materials composed of only S-shaped resonators, *Phys. Rev. E* 70 (2004) 0576051–0576054.
- [7] O. Luukkonen, S.I. Maslovski, S.A. Tretyakov, A stepwise Nicolson–Ross–Weir-based material parameter extraction method, *IEEE Antennas Wirel. Propag. Lett.* 10 (2011) 3588–3596.